JOURNAL OF GEOPHYSICAL RESEARCH, VOL. 113, C07S90, doi:10.1029/2007JC004547, 2008

Vertical stability and the annual dynamics of nutrients and chlorophyll fluorescence in the coastal, southeast Beaufort Sea

Jean-Éric Tremblay,[1,2] Kyle Simpson,[1] Johannie Martin,[2] Lisa Miller,[3] Yves Gratton,[4] David Barber,[5] and Neil M. Price[1]

Received 11 September 2007; revised 15 February 2008; accepted 29 February 2008; published 9 July 2008.

[1] The first quasi-annual time series of nutrients and chlorophyll fluorescence in the southeast Beaufort Sea showed that mixing, whether driven by wind, local convection, or brine rejection, and the ensuing replenishment of nutrients at the surface were minimal during autumn and winter. Anomalously high inventories of nutrients were observed briefly in late December, coinciding with the passage of an eddy generated offshore. The concentrations of NO_3^- in the upper mixed layer were otherwise low and increased slowly from January to April. The coincident decline of NO_2^- suggested nitrification near the surface. The vernal drawdown of NO_3^- in 2004 began at the ice-water interface during May, leaving as little as 0.9 μM of NO_3^- when the ice broke up. A subsurface chlorophyll maximum (SCM) developed promptly and deepened with the nitracline until early August. The diatom-dominated SCM possibly mediated half of the seasonal NO_3^- consumption while generating the primary NO_2^- maximum. Dissolved inorganic carbon and soluble reactive phosphorus above the SCM continued to decline after NO_3^- was depleted, indicating that net community production (NCP) exceeded NO_3^- -based new production. These dynamics contrast with those of productive Arctic waters where nutrient replenishment in the upper euphotic zone is extensive and NCP is fueled primarily by allochthonous NO_3^-. The projected increase in the supply of heat and freshwater to the Arctic should bolster vertical stability, further reduce NO_3^- -based new production, and increase the relative contribution of the SCM. This trend might be reversed locally or regionally by the physical forcing events that episodically deliver nutrients to the upper euphotic zone.

Citation: Tremblay, J.-É., K. Simpson, J. Martin, L. Miller, Y. Gratton, D. Barber, and N. M. Price (2008), Vertical stability and the annual dynamics of nutrients and chlorophyll fluorescence in the coastal, southeast Beaufort Sea, *J. Geophys. Res.*, *113*, C07S90, doi:10.1029/2007JC004547.

1. Introduction

[2] Winds and convection during autumn and winter erode the weak vertical stratification every year in the North Atlantic and Pacific oceans, thereby replenishing the stock of macronutrients for primary producers in the euphotic zone. In the coastal Beaufort Sea, however, the imports of freshwater from rivers and low-salinity water from the Bering Sea promote a strong halocline that stabilizes the upper water column [*Carmack and Wassmann*, 2006]. Fast ice provides a shield against wind-driven mixing and upwelling during winter, and ice melt augments stratification during summer. The impacts of global warming and climate forcing on vertical stratification, sea ice and the freshwater balance in the Arctic Ocean are under close scrutiny [e.g., *Peterson et al.*, 2006], but consequences for critical ecosystem functions such as nutrient loading and primary production are poorly constrained.

[3] Recent studies suggest that nitrogen supply is the primary control of the net, annual yield of primary producers in seasonally ice-covered waters of the Arctic Ocean, whereas irradiance and algal physiology interact to set the timing, species composition and fate of the main production pulse(s) [*Tremblay et al.*, 2002b, 2006b; *Walsh et al.*, 2004]. Physical regime shifts thus hold the potential to alter biogeochemical fluxes and the success of the renewable resources that depend on micro-algal production [*Tremblay et al.*, 2006a; *Walsh et al.*, 2004].

[4] Nutrients are supplied to the upper Arctic Ocean by a variety of processes operating at different spatial and temporal scales. At the periphery, large-scale horizontal inputs are provided by rivers and advection from marginal seas. The residence time of these waters in the Arctic is of the order of a decade, and unless they transit exclusively

[1]Department of Biology, McGill University, Montréal, Québec, Canada.
[2]Département de Biologie et Québec-Océan, Université Laval, Québec City, Québec, Canada.
[3]Institute of Ocean Sciences, Fisheries and Oceans Canada, Sidney, British Columbia, Canada.
[4]INRS-ETE, Québec City, Québec, Canada.
[5]Centre for Earth Observation Science, University of Manitoba, Winnipeg, Manitoba, Canada.

0148-0227/08/2007JC004547$09.00

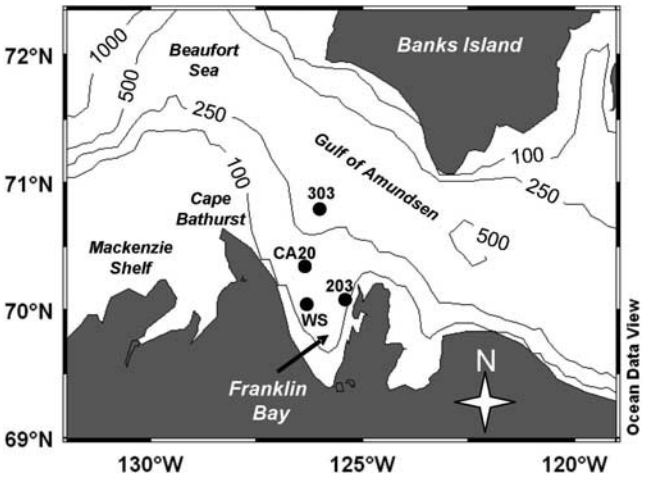

Figure 1. Map of the southeast Beaufort Sea and the Gulf of Amundsen showing the position of the owerwintering site (WS), the mooring site (CA20), and two other stations considered in the present paper (203 and 303).

under thick ice, labile nutrients are consumed close to their source during the first year. It follows that, in the interior, nutrient renewal depends on upward supply from intermediate waters, which is conditioned by the overall strength and resilience of the halocline. The latter is presumably increasing with the ongoing rise in air temperature and freshwater discharge [*Peterson et al.*, 2006], further reducing the mean, upward flux of nutrients. Against this backdrop, physical singularities episodically subsidize a given region with nutrients. These singularities can take the form of internal waves, storms that erode the halocline, shelf-break upwelling and dynamic instabilities caused by topography or convection [*Mathis et al.*, 2007; *Williams et al.*, 2006; *Zhang et al.*, 2004; *Tremblay et al.*, 2002b]. The incidence and strength of upwelling events and halocline perturbations are presumably increasing with the rising frequency and intensity of cyclones [*Yang et al.*, 2004] and the retreat of the perennial ice pack beyond the shelf break [*Carmack and Chapman*, 2003].

[5] It is not currently possible to assess or forecast the net result of changes in the mean versus episodic deliveries of nutrients on the magnitude and species composition of primary production. While the physical processes conducive to nutrient renewal are reasonably well understood, the actual fluxes of nutrients are seldom quantified and compared with concurrent processes such as biological assimilation and recycling. The most basic time series of nutrients and phytoplankton biomass are lacking and we have no reference by which the impact of climate change can be measured. The scant, published information on nutrients during late fall and winter in the Beaufort Sea was obtained from drift stations, e.g., the T3 ice island which intersected different water masses and physiographic regions. Although valuable, these data do not constitute a temporal sequence and, to our knowledge, none exist for the coastal Beaufort Sea. An Eulerian approach is needed to document the relative influence of external supply versus regional physical and biological processes in controlling nutrient availability, new production (i.e., the portion total primary production derived from the uptake of allochthonous nitrogen) and net community production (NCP; the production of carbon in excess of community metabolism) in the coastal zone.

[6] During 2003 and 2004, the Canadian Arctic Shelf Exchange Study program (CASES) produced the first time series of vertically resolved nutrient concentrations and chlorophyll fluorescence at a fixed overwintering site located at the southeast margin of the Beaufort Sea (Franklin Bay). Here we present and discuss this time series in relation to ancillary physical and fluorescence data recorded at a nearby moored observatory.

2. Methods

2.1. General

[7] All samples were obtained during the 2003–2004 expedition of the Canadian Coast Guard Ice Breaker CCGS *Amundsen*. From October to December 2004, the ship completed a broad survey of the open waters of the southeastern Beaufort Sea and Mackenzie Shelf (Figure 1). During this mobile phase, the ship sampled in Franklin Bay on 12 October (station CA20) and 4 and 19 November (overwintering site (WS)). The ship was subsequently iced-in and sampled at the 230-m-deep WS between 10 December 2003 and 27 May 2004. On 1 June 2004 the ship broke free and sampled in the Gulf of Amundsen (e.g., station 303) before revisiting the WS on 16 July and 6 August. Nearby stations CA20 and 203 were sampled on 21 June and 2 August, respectively.

[8] Vertical profiles of nutrients, dissolved inorganic carbon (DIC), temperature, salinity and fluorescence were obtained with a rosette equipped with 24 12-L Niskin bottles, a CTD (Seabird SBE-911) and a fluorometer (Sea-Point). Depending on ice conditions, the rosette was deployed alongside the ship or through the internal moon pool. During the freeze-in, vertical profiles of physical parameters and fluorescence were obtained twice a day, whereas nutrient and DIC samples were collected every sixth day between 10 December 2003 and 15 May 2004, and then every third day until 27 May. Standard depths of collection were 10, 15, 25, 50, 75, 100, 125 (or the depth corresponding to a salinity of 33.1, which marks the Si maximum), 150, 175, 200 and 225 m (DIC samples were not taken at 10, 15 and 25 m when sampling was conducted through the moon pool). Matching surface samples (3 and 10 m) were collected with GOFLO (nutrients) and Kemmerer (DIC) bottles at an ice camp located a few hundred meters off the ship. When the ship was mobile additional samples were taken in the euphotic zone. At station CA20, a fluorometer (Alec CLW) attached at 30 m on a mooring provided a semicontinuous record of chlorophyll fluorescence from October 2003 to mid-July 2004.

2.2. DIC

[9] Dissolved inorganic carbon was determined by coulometric titration [*DOE*, 1994] with a SOMMA instrument [*Johnson et al.*, 1993] fit to a UIC 5011 coulometer and calibrated against certified standards (CRM Batch 61, provided by Andrew Dickson of the Scripps Institute of Oceanography) and a secondary standard which was regularly calibrated directly against CRM Batch 61. Precision,

based on the difference between two replicate samples drawn from the same Niskin bottle varied between legs from 1.6 to 3.9 μmol/kg. In order to compensate for the effect of ice melt on DIC concentrations, data obtained later during summer were standardized to the spring salinity profile (i.e., corrected DIC = observed DIC $\times$ spring salinity/observed salinity at depth z) in order to correct for the dilution imparted by ice melt. The dynamics of DIC during autumn and winter will be discussed in detail elsewhere and the present analysis is restricted to the spring-summer period.

2.3. Nutrients

[10] Nutrients were collected in acid-washed 15-mL PP tubes. Large particles were removed by inline filtration through a 5.0 μm polycarbonate filter mounted on a 47-mm filter holder and attached directly to the sampling bottles. This procedure was preferred over the classical syringe and GF/F method in order to minimize handling and contamination. Samples collected prior to 10 December 2003 and after 27 May 2004 were analyzed fresh, and those collected during the overwintering period were quickly frozen and stored at -20°C. Frozen samples were rapidly thawed in a tepid water bath, thoroughly mixed and analyzed immediately during mid-May 2004. Colorimetric determinations of $NO_3^- + NO_2^-$, NO_2^- and of soluble reactive phosphorus and silicate (hereafter abbreviated as P and Si, respectively) were performed on an Autoanalyzer 3 (Bran and Luebbe) with routine methods adapted from *Grasshoff* [1999]. Analytical detection limits were 0.03 μM for $NO_3^- + NO_2^-$, 0.05 and 0.1 μM for P and Si, respectively, and 0.02 μM for NO_2^-. In order to test for the effect of sample freezing on nutrient determinations, a subset of samples were analyzed fresh in mid-April, stored frozen and analyzed again in mid-August. No bias was detected.

2.4. Fluorescence

[11] The output of the Rosette fluorometer was calibrated against extracted chlorophyll-*a* (chl *a*) (fluorometric method; data courtesy of S. Brugel) between April and August 2004. The best fit (n = 124; $r^2 = 0.91$) was provided by a quadratic polynomial model and indicated that the fluorescence yield of chl *a* decreased with increasing biomass. This relationship was used to convert fluorescence to chl *a* biomass in order to take advantage of the high-resolution Rosette data during winter and spring at the WS. No similar conversion was attempted with the moored fluorometer, whose data are reported as relative units.

2.5. Physics

[12] Density was calculated from the temperature and salinity data obtained with the CTD (salinity was checked against direct determination with a Guildline Autosal salinometer). The Brunt-Vaisala frequency (N^2) was calculated from the density gradient [*Pond and Pickard*, 1978] and used to locate the pycnocline on individual profiles.

3. Results

3.1. Stratification and Nutrients at the WS

[13] The composite time series of measurements in Franklin Bay is shown in Figure 2. In general, the main pycnocline (i.e., maximum value of N^2) was shallow and persisted throughout the entire window of observation. A secondary, vertical peak in N^2 was observed at ca. 160 m, marking the transition between Pacific-derived water and the deep Atlantic layer. The main pycnocline deepened in late November and early December when the fast ice consolidated, but shoaled radically on 22 December. The deep expression of this anomaly occurred a few days later with the pronounced uplifting of the deep N^2 peak to ca. 80 m. A lasting, albeit weaker pycnocline soon reappeared and exhibited vertical excursions between 15 and 45 m.

[14] During autumn 2003, concentrations of NO_3^- were initially low (<0.5 μM) in the upper 20 m and showed a small increase in late November and early December. The highest surface concentration (5.7 μM) of the time series was observed on 22 December, coincident with the surface expression of the N^2 anomaly. Surface concentrations declined immediately afterward and ranged from 3.3 μM to 0.9 μM until the end of May. The nitracline tracked the pycnocline, and the lowest concentrations of NO_3^- in the upper 40 m corresponded to the deepest mixed layers. A clear seasonal deficit was visible in the upper 20 m on 16 June and concentrations reached the analytical detection limit (<0.03 μM) near the surface. Concentrations of nitrite were generally high in late 2003 (max 0.43 μM), with a primary maximum that shoaled from 50 m in November to 15 m in December, respectively. The primary maximum vanished during winter, reappeared in June 2004 at 25 m (0.15 μM) and deepened to 40 (0.10 μM) and 46 m (0.27 μM) in July and August, respectively.

[15] In the upper 40 m, the concentrations of P and Si followed the same qualitative pattern as NO_3^-, but generally remained in substantial excess when NO_3^- was depleted. Unusually low values (0.45 μM for P and nondetectable Si) were observed on 21 July. In contrast with NO_3^-, P and Si showed a deep maximum, generally close to 150 m, which typically marks the presence of modified Pacific water propagating with the lower halocline. This maximum was unusually shallow during the late December N^2 anomaly, when waters with the high NO_3^-/P and low Si/NO_3^- ratios typical of the deep Atlantic layer were seen at 100 m, more than 50 m above their usual position. Near the surface, extremely low NO_3^-/P (≤ 2) and high Si/NO_3^- ($5 - \infty$) ratios during autumn 2003 and summer 2004 reflected the excess of P and Si after the near exhaustion of NO_3^-. The low Si/NO_3^- and high NO_3^-/P typical of intermediate waters were seen near the surface on 22 December only. Otherwise, Si/NO_3^- and NO_3^-/P did not approach the values observed beneath the pycnocline, ranging from 2.8 to 4.0 and from 2.0 to 4.0, respectively. Temporal variability was most pronounced at ca. 25 m, where packets of water with high and low Si:N ratios alternated. Kernels of low Si/NO_3^- coincided with relatively shallow mixed layers.

[16] The details of the different water types observed in the upper water column are shown in Figure 3. The water associated with the N^2 anomaly of 22 December was relatively warm, saline and exhibited relatively high concentrations of NO_3^- and low Si/NO_3^- ratios in the upper 30 m. These features were observed at other times when the pycnocline was shallow but were not as pronounced (e.g., 3 March). The water type characterized by relatively deep pycnoclines (e.g., 3 February and 27 March) was

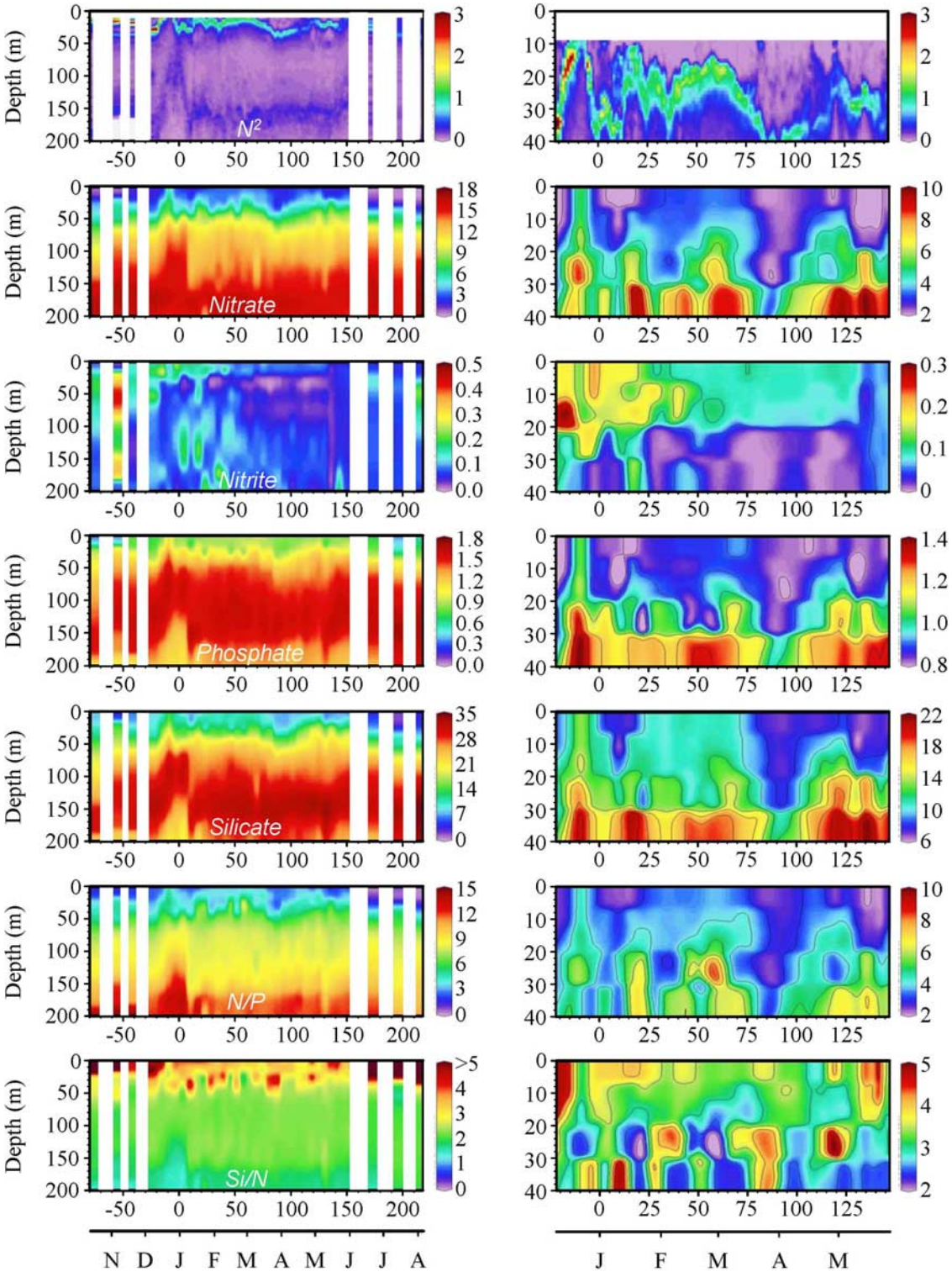

Figure 2. Composite time series of the Brunt-Vaisälä frequency (N^2; $\times 10^{-3}$ s^{-2}), NO_3^-, nitrite, P, and Si (all in μM) and the ratios NO_3^-/P and Si/NO_3^- at the WS (4 November 2003 to 27 May 2004; 16 July and 6 August 2004) and at nearby sampling sites (12 October, 21 June, and 2 August). The right-hand side is a close-up on the upper 40 m of the high-resolution WS data from 10 December 2003 to 27 May 2004 (sampling frequency was every 6th day until 15 May and every third day afterward). Depths of sample collection are not marked to avoid clouding the images, but see details in section 2.1. This figure was prepared with the Ocean-Data-View software (R. Schlitzer, http://odv.awi.de).

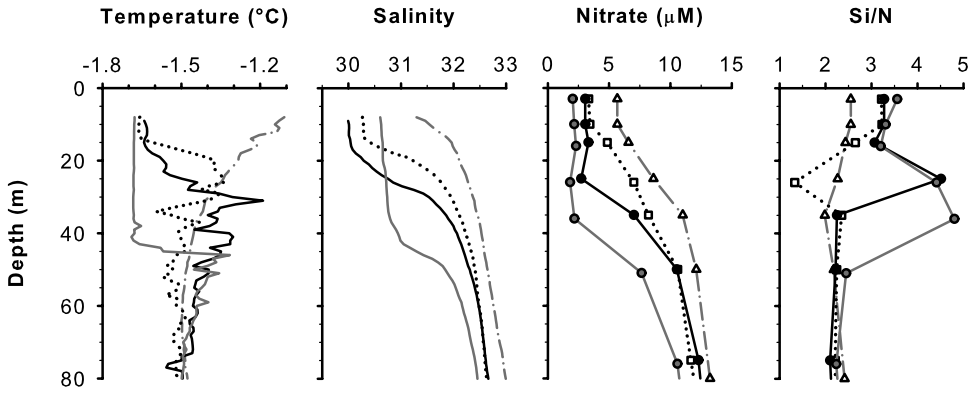

Figure 3. Characteristics of the main water masses observed during late fall 2003 and winter 2004 at the WS. Sampling dates characterized by relatively shallow pycnoclines are represented by open symbols (22 December given by dash-dot lines and triangles; 3 March given by dotted lines and squares) and those characterized by relatively deep pycnoclines and subsurface maxima in temperature and Si/N are represented by closed symbols (3 February given by black lines and circles; 27 March given by gray lines and circles).

relatively fresh, cold and poor in NO_3^- in the upper 30 m. It showed a distinct temperature maximum at the pycnocline (up to −1.19°C on 3 February) that coincided with peaks in Si/NO_3^-.

[17] To account for the changing water types in our analysis of local events, the winter sampling dates for which the pycnocline was one standard deviation above or below the long-term average were filtered out of the time series. The mean, weighted concentration of each nutrient above N^2_{max} was then calculated. This subset of data showed a gradual increase in NO_3^- at the mean rate of 13.2 ± 2.5 nmol d^{-1} ($r^2 = 0.68$) until mid-March (Figure 4). Concentrations eventually leveled off and then decreased from May to August. Concentrations of NO_2^- increased until late December and then steadily decreased at a mean rate of 1.4 ± 0.3 nmol d^{-1} ($r^2 = 0.66$) until mid-March, after which values remained low and fairly constant. In contrast with NO_3^-, most of the increase in P and Si occurred in late 2003. During winter, no significant increase in Si was observed and the rising trend in P (1.0 ± 0.4 nmol d^{-1}; $r^2 = 0.33$) was barely significant, yielding an estimated NO_3^-/P build-up ratio of 13.2 ± 5.8.

3.2. Chlorophyll at the WS and Fluorescence at the Mooring Site

[18] Chlorophyll biomass was moderate at the beginning of the time series, with maximum values of ca. 0.5 μg L^{-1} in the upper 20–30 m during the fall bloom (Figure 5). Concentrations then decreased until mid-January and remained extremely low (<0.04 μg L^{-1}) until late February. Near the surface, there was a slow and progressive increase to 0.31 μg L^{-1} on 11 May (0.31 μg L^{-1}), prior to the onset of ice melt. The highest concentrations of the time series (maximum of 2.5 μg L^{-1}) were observed later in the season within the subsurface chlorophyll maximum (SCM). Total water column inventories at the WS rose from a minimum of 5.3 mg m^{-2} in February to 6.9 and 55 mg m^{-2} on 27 May and 21 July, respectively, after which they declined to 37 mg m^{-2} on 6 August. High-resolution fluorescence data from the nearby mooring site (CA20) showed a steep rise of chlorophyll fluorescence at 30 m on 3 June, less than 15 days after the ice began clearing the bay. The signal exhibited large fluctuations and persisted at least until mid-July, when the instrument stopped recording.

[19] Relationships between the SCM, NO_3^- and nitrite during spring and summer 2004 are explored in Figure 6. The SCM had not yet appeared when the ship left the WS station on 27 May but was present at every subsequent sampling occasion, deepening from 32 m on 16 June (max 2.5 μg L^{-1}) to 57 m on 6 August (max 2.2 μg L^{-1}). The vertical distribution of chl *a* in the SCM was remarkably broad on 16 July and coincided with the highest water column inventory of the time series. The primary nitrite maximum generally gained in intensity and deepened along with the SCM and the nitracline during summer.

3.3. Drawdown of Nutrients and DIC During 2004

[20] The absolute drawdown of nutrients in polar waters can be estimated by computing the difference between observed nutrient concentrations and conservative expectations based on salinity at the core of the relevant water mass [e.g., *Wallace et al.*, 1995]. In Figure 7, the solid circles and lines correspond to the stations where the highest concentrations of nutrients or DIC were observed as a function of salinity between March and May, which we take as a reference. The dashed lines show what the concentrations would be if the properties were diluted conservatively with salt above 75 m. It is obvious that a substantial nutrient deficit persisted throughout the winter in surface water and that it was more pronounced for NO_3^- and Si than for P. Surface DIC, on the other hand, was higher than conservative expectations. In Figure 7, departures from the reference property-salinity relationship (solid line) indicate seasonal biological drawdown or mineralization.

[21] For the estimation of net NO_3^- deficits, the salinity profiles obtained in late spring and summer were used to produce reference NO_3^- profiles from the baseline relationship of 15 March (Figure 8). Conservative dilution was assumed at lower salinities in order to correct for freshwater inputs (e.g., ice melt). The deeper part of the reference and observed profiles matched perfectly except on 6 August, when NO_3^- concentrations below 60 m exceeded those

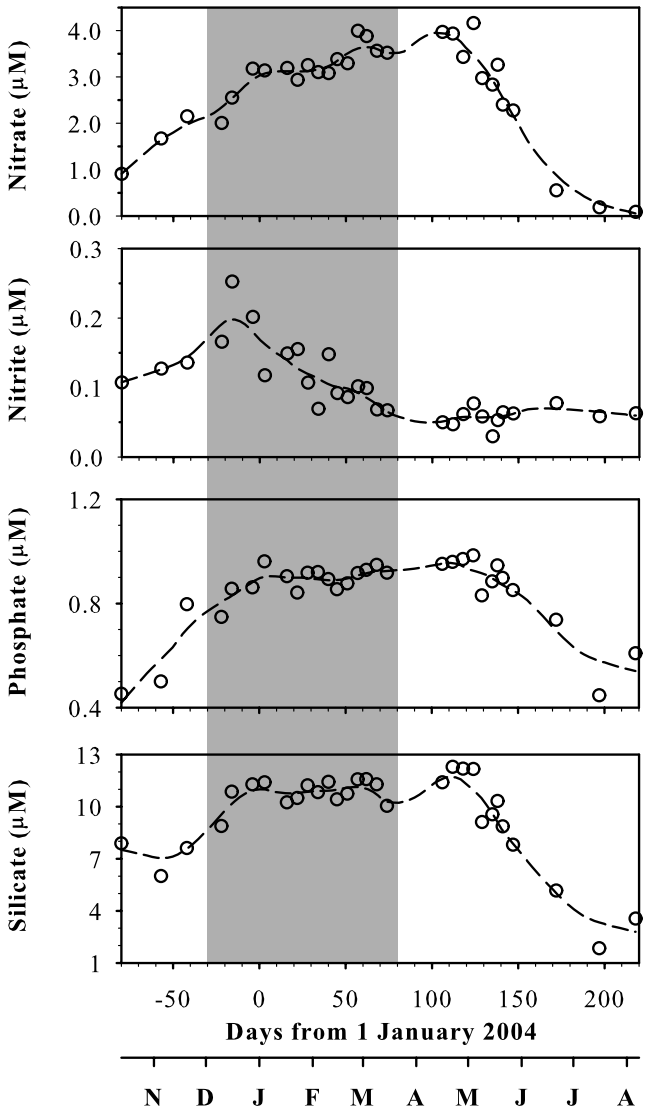

Figure 4. Time series of the mean concentrations of NO_3^-, NO_2^-, P, and Si above the pycnocline. The dashed line is a running average and the shaded area indicates the period between the establishment of the fast ice cover in 2003 and the onset of rapid ice algal growth in late March 2004 [see *Riedel et al.*, 2006].

predicted by the reference profile. This discrepancy implies recent mineralization or the passage of a different water mass at the WS. The latter is more plausible since the discrepancy extended all the way to the bottom (not shown) and so we corrected the reference profile by normalizing it to the NO_3^- concentration at 100 m. Net deficits at the WS were calculated from the difference between observed and reference inventories in the upper 75 m, yielding 22, 114 and 211 mmol NO_3^- m^{-2} on 27 May, 16 July, and 6 August, respectively. Estimates for stations CA20 (21 June) and 203 (2 August) were 138 and 171mmol NO_3^- m^{-2}, respectively. In all cases the NO_3^- deficit extended well below the main pycnocline. We did not attempt to estimate NCP directly from changes in DIC concentrations due to the low vertical resolution of sampling in the upper 50 m and the uncertainty attached to air-sea flux.

[22] Drawdown ratios of the different nutrients and DIC between 28 April and 6 August 2004 were established using data from the upper 75 m only since no net depletion was apparent below this horizon (Figure 9). Although nutrient data were obtained at a higher resolution than DIC data in the upper 50 m, only the sampling depths at which DIC information was available were considered in order to obtain a coherent set of ratios. Given the obvious vertical disconnect of DIC and nutrient renewal processes evidenced in Figure 7, DIC and nutrient data were not normalized to a constant, core salinity but instead to vertically matching salinities on 27 May. Drawdown ratios were taken as the slopes of model II (or geometric mean) linear regressions using the data points for which NO_3^- concentration exceeded 0.5 μM (circles in Figure 9). The resulting C:N:P stoichiometry of drawdown for this subset of data was 102:14:1, with a corresponding Si:NO_3^- ratio of 1.86. The latter was much higher than previously observed in other waters of Canada Basin provenance (1.01; *Tremblay et al.* [2002a]). Despite the small number of data points at low concentrations, Figure 9 implies that the drawdown of P and Si continued after NO_3^- was nearly exhausted and that P was depleted even further once Si was no longer available on 21 July (gray squares in Figure 9 and diamonds in Figure 7). The standardized DIC data for that period are few and noisy, possibly because of variable air-sea exchange and respiration, but suggests that extra NCP matched the additional P consumption.

4. Discussion

[23] The present data set constitutes the first time series of nutrients and chlorophyll fluorescence from autumn to summer in the coastal Beaufort Sea. The most salient result was the very modest replenishment of nutrients during autumn and winter, which contrasts with other peripheral Arctic seas and the coastal Southern Ocean [e.g., *Tremblay and Smith*, 2007; *Wassmann et al.*, 1999]. The causes and implications of this result will now be discussed in detail with respect to (1) the transient increase, or anomaly, in nutrient inventories during late December 2003; (2) the apparent decoupling in the renewal of NO_3^- and P versus Si during winter; (3) changes in nitrite concentrations; and (4) the contribution of NO_3^- to new and net production. Given the absence of similar time series from the literature, our time series can only be compared with that of the eastern North Water Polynya, where late winter nutrient concentrations were also measured in Pacific-derived waters [*Tremblay et al.*, 2002a].

4.1. Mechanisms of Nutrient Supply to the Euphotic Zone

4.1.1. Physical Processes

[24] Apart from autumn 2003 when surface salinities were sometimes as low as 23.5 (not shown), freshwater plumes were not detected at the WS. Their influence must vanish during winter when freshwater from the Mackenzie River is contained in a neritic lake by the stamukhi [*Carmack and MacDonald*, 2002] and the Horton River is frozen to the bottom. There was no evidence of a spring

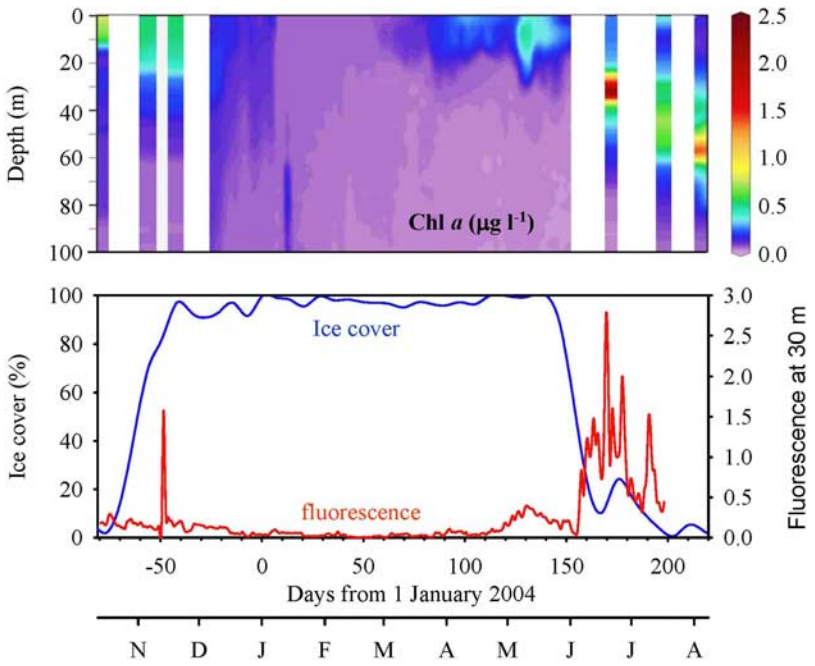

Figure 5. Time series of (top) chl *a* estimated with the Rosette-mounted fluorometer at the WS (sampling frequency was twice daily during the freeze-in period) and nearby sampling sites and (bottom) the mean extent of fast ice in Franklin bay (blue line) and the fluorescence (red line, arbitrary units) at 30 m at the mooring site CA20. Figure 5 was prepared with the Ocean-Data-View software (R. Schlitzer, http://odv.awi.de).

freshet either (Y. Gratton, personal communication, 2007), which is not surprising since winds must be strong and blow from the northwest to drive the Mackenzie plume around Cape Bathurst and to the WS (Figure 1). The presence of strong pycnoclines throughout October and November implies that wind-driven mixing was weak in 2003 despite the episodic passage of mild storms over the area. This limited mixing, which apparently injected nutrients into the

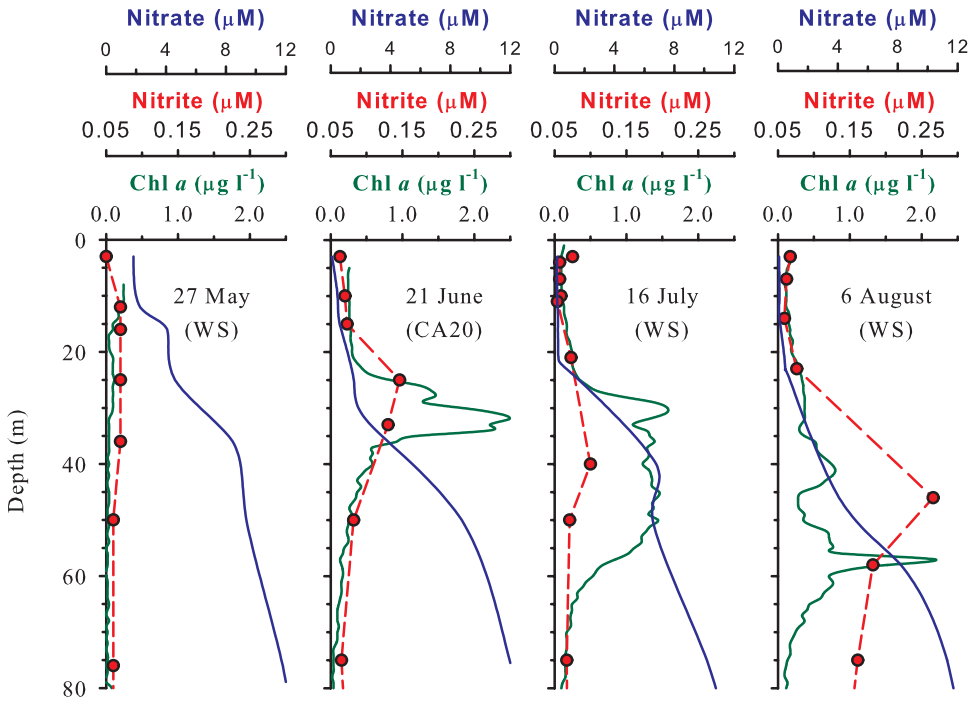

Figure 6. Vertical profiles of NO_3^- (blue lines), nitrite (red circles and dashed lines), and chl *a* (green lines) at the WS (27 May, 16 July, and 6 August 2004) and station CA20 (21 June 2004).

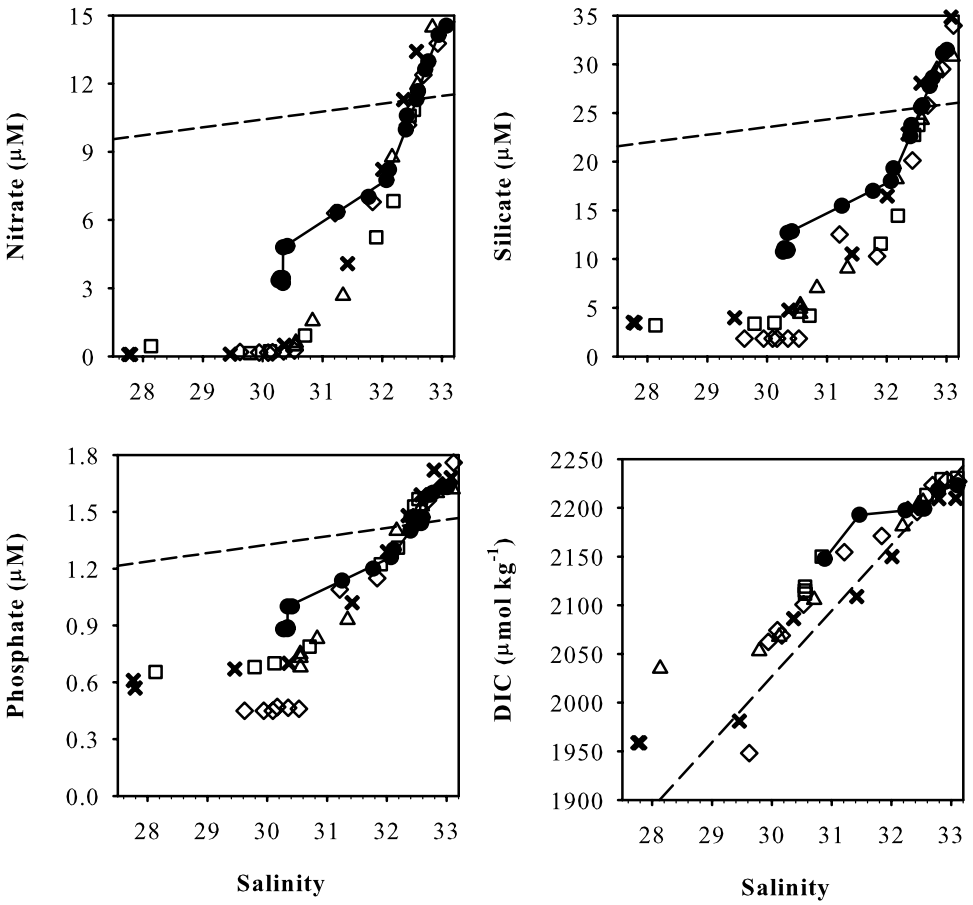

Figure 7. Plots of NO_3^-, P, Si, and dissolved inorganic carbon (DIC) against salinity for the winter baseline (lines and closed circles) and on 21 June (squares), 16 July (diamonds), 2 August (triangles), and 6 August (crosses). The dashed line indicates what the concentrations would be if they were diluted conservatively with salinity above 75 m.

upper euphotic zone and drove the modest autumn bloom, must have been halted with the consolidation of fast ice in December (Figure 5). Convection and brine rejection were necessary to drive the deepening of the pycnocline during the first 10 days of December and the concomitant increase in NO_3^-, P and Si near the surface (Figure 4). The resultant mixing was very incomplete, however, as indicated by the persistence of high Si/NO_3^- ratios, which carry the signature of biologically spent water in the upper mixed layer (Figure 2). The coincidence of subsurface kernels of high Si/NO_3^- and temperature maxima in the water mass characterized by relatively deep pycnoclines during winter

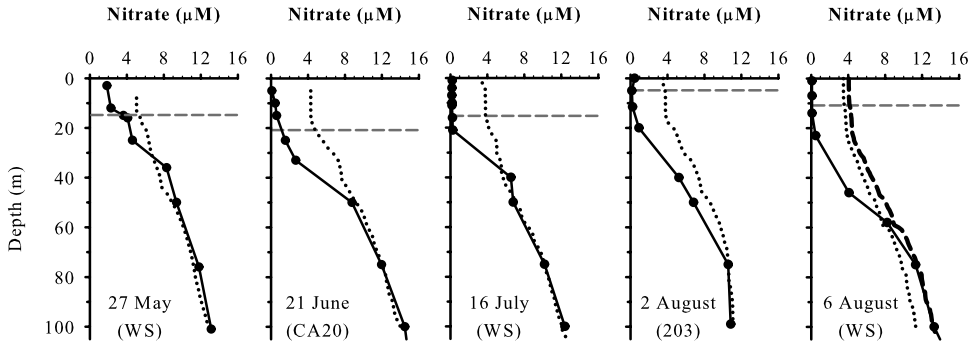

Figure 8. Vertical profiles of observed (solid lines and closed circles) and reference (dotted lines, inferred from observed salinity and the winter baseline relationship between NO_3^- and salinity) concentrations of NO_3^- at the WS (27 May, 16 July, and 6 August) and nearby locations (21 June and 2 August). The horizontal dashed lines mark the pycnocline, and the vertical dashed line on 6 August marks the reference profile corrected for the apparent shift in water masses (see section 3.3).

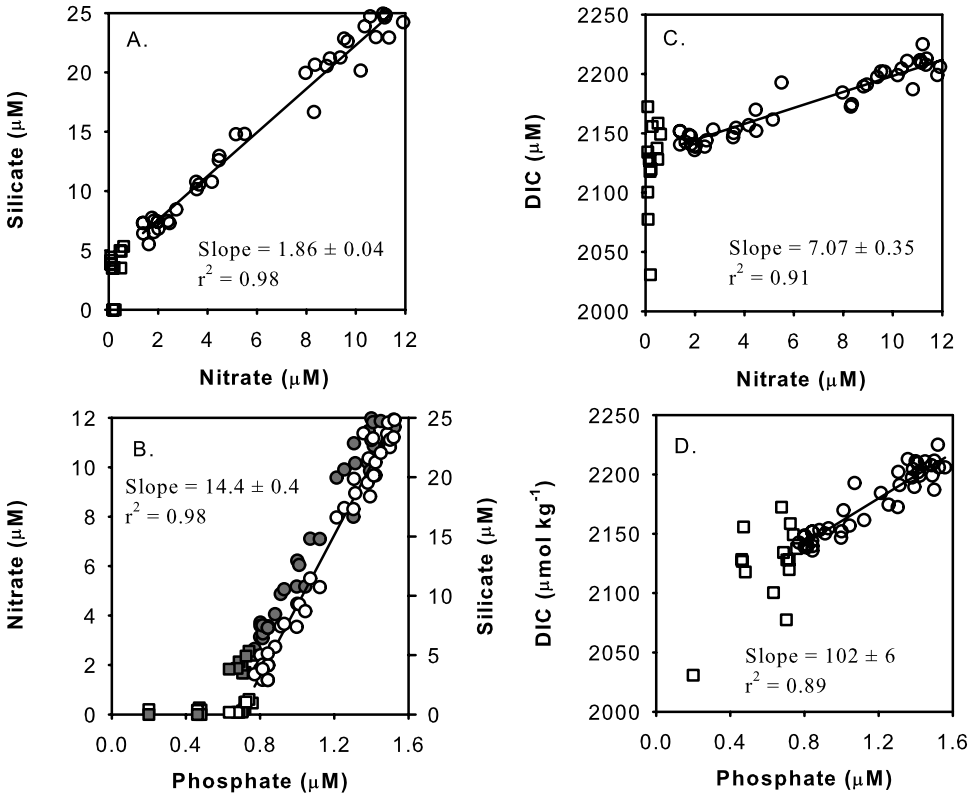

Figure 9. Plots of (a) Si against NO_3^-, (b) NO_3^- against P (open symbols and regression line) and Si against P (closed symbols), (c) DIC against NO_3^-, and (d) DIC against P for samples taken at and above 75 m and for which NO_3^- concentrations were greater (circles) or lower (squares) than 0.5 μM. The lines, their slopes, and r^2 values are for model II (geometric mean) regressions. Nutrient and DIC data collected from 21 June onward were corrected for freshwater dilution on the basis of the salinity profile observed immediately prior to ice melt (27 May).

confirms that convection was generally limited to the upper 30 m, except during late March and early April when the mixed layer was unusually deep (Figures 2 and 3).

[25] Two lines of evidence show that the elevated nutrient concentrations observed on 22 December were not generated locally. First, the total water column inventories of salt and nutrients far exceeded those observed at any other time or location in the bay (Figure 3; see also Y. Gratton, personal communication, 2007). For the same reason, this water cannot have come around Cape Bathurst from the shallow, Mackenzie Shelf and must have originated at or beyond the shelf break. The passage of a deep anticyclonic eddy through the WS is the most likely scenario and is consistent with the time lag between the surface and deep expressions of the anomaly (Figure 2); that is, the shallow outer edge of an eddy would pass through the WS before its deep inner core (Y. Gratton, personal communication, 2007). It is still not clear whether we had a hedon-type vertical dipole [*Chao and Shaw*, 1996]. A shallow brine source can generate a deep anticyclonic eddy coupled to a smaller surface cyclonic eddy strongly affected by the ice friction. The point of origin of this eddy-like feature cannot be determined but it was possibly generated in the adjacent Cape Bathurst Polynya, which is more prone to atmospheric forcing than the fast ice laden Franklin Bay. An eddy could also have been generated by the dynamical instability resulting from deep convection and its interaction with the shelf break (Y. Gratton, personal communication, 2007) [see also *Marshall and Schott*, 1999]. The warm surface temperatures on 22 December (−1.1°C) relative to the bracketing time points (−1.6°C) lend further support to this hypothesis (Figure 3). Such a warm anomaly requires the continual, upward mixing of heat and is inconsistent with long-range Ekman drift (of waters upwelled elsewhere) or an intrusion of the Beaufort shelf-break jet [*Pickart*, 2004]. The hull-mounted ship ADCP recorded relatively strong currents from −25 to +20 cm s^{-1} during the anomaly, with the current changing direction on 25 December. Apart from this event, which delivered the highest NO_3^- concentrations of the time series (up to 5.7 μM at surface), the physical renewal of nutrients in autumn and winter was weak.

4.1.2. Biological Processes

[26] Beyond the noise imparted by changing water mass characteristics, the mean concentration of Si in the upper mixed layer was nearly invariant after December, whereas NO_3^-, and to a lesser extent P, increased until spring (Figure 4). Such decoupling suggests that the renewal of NO_3^- and P was not strictly physical, otherwise mixing and upward diffusion across the pycnocline would also replenish Si. Assuming that NO_3^- was not consumed in near-absolute darkness under thick ice, the net increase of 13.2 nmol N d^{-1} in NO_3^- during winter was probably

driven by bacterial or archeal nitrification above the pycnocline. The coinciding decline of NO_2^- concentrations at the mean rate of 1.4 nmol N d^{-1} indicates that nitrification of the NO_2^- already present in early winter would have supplied 11% of the net increase in NO_3^-. Erosion of the primary NO_2^- maximum due to modest mixing during late fall brought the required NO_2^- to the surface (Figures 2 and 4). The concurrent increase in P was presumably supplied by the decomposition of dissolved organic phosphorus (DOP), which accumulated during the productive season and declined during autumn and winter [*Simpson et al.*, 2008].

[27] The seasonal increase in NO_2^- inventories and development of the primary maximum we observed in Franklin Bay appears to be generalized in the southeast Beaufort Sea (K. Simpson et al., Nutrient dynamics in the Amundsen Gulf and Cape Bathurst Polynya: 1. New production in spring inferred from nutrient draw-down, submitted to Marine Ecology Progress Series, 2008.). On the vertical, the association between the nitrite maximum, the SCM and the nitracline (Figure 6) strongly suggests that the NO_2^- was released by phytoplankton, possibly because irradiance at the SCM was not always sufficient to drive the complete reduction of NO_3^- or because shade-adapted algae used NO_3^- reduction as an electron sink when transiently exposed to higher light intensities [*Lomas and Glibert*, 1999]. Phytoplankton are hypothesized to be the principal cause of formation and maintenance of the primary nitrite maximum in other stratified oceans (see references given by *Lomas and Lipschultz* [2006]), which is even more likely in the Beaufort Sea where the maximum is shallow enough for light to inhibit NH_4^+ oxidizers during summer [e.g., *Guerrero and Jones*, 1996]. If this is true, then the NO_3^- produced by the wintertime nitrification of the NO_2^- released in the primary nitrite maximum during summer should be considered allochthonous and not recycled, since the N was not assimilated into biomass.

[28] The major portion (89%) of the net wintertime increase in NO_3^-would have to be driven by NH_4^+ oxidation without any net accumulation of NO_2^-, implying a similar rate for the two reactions. Nitrification measurements performed in other regions support this scenario [*Yool et al.*, 2007; *Ward*, 2002]. The amount of NH_4^+ needed to drive the NO_3^- increase for 110 days was 1.3 μM, which could be supplied by the standing inventory of NH_4^+ in autumn 2003 (mean concentration = 1.5 μM in the upper 50 m in early November; K. Simpson, personal communication, 2007) and the ammonification of dissolved organic nitrogen (DON) to NH_4^+ by microbial heterotrophs during winter. Both pathways are consistent with the seasonal build-up of NH_4^+ and DON inventories during summer and their subsequent decrease during winter and early spring [*Simpson et al.*, 2008]. Furthermore, *Nitrosospira*- and *Nitrosomonas*-like bacteria with NH_4^+−oxidase activity were previously reported in the central Arctic [*Hollibaugh et al.*, 2002] and potentially nitrifying archea and bacteria were present in the surface waters of Franklin Bay [*Wells et al.*, 2006; *Garneau et al.*, 2006]. The required, mean NH_4^+ oxidation rate of 11.8 nmol N d^{-1} is an order of magnitude lower than measured rates for the warm, oligotrophic Pacific Ocean [*Dore and Karl*, 1996] but similar to the rates measured in the cold waters of the Southern Ocean [*Bianchi et al.*, 1997]. The nitrification hypothesis remains to be tested, but our results show that biological processes in the coastal Arctic may have a large impact on NO_3^- dynamics in the absence of strong physical forcing.

4.2. Subsurface Chlorophyll Maximum

[29] When under-ice phytoplankton or sloughed ice algae become exposed to high irradiance, they typically show severe photoinhibition. Results from the North Water indicate that it may take up to two weeks before surface communities of phytoplankton fully adjust to incident irradiance [*Tremblay et al.*, 2006b]. In Franklin Bay, the availability of NO_3^- may place an additional constraint on growth rates at the surface. During the second half of May, before the ice cleared, the concentration of NO_3^- at the ice-water interface ranged from 2.0 to 0.9 μM (Figures 2 and 8) as a result of the early algal growth observed at low light intensity underneath the ice (Figure 5). Reported half-saturation constants for NO_3^- uptake in Arctic waters range from 0.9 to 2.2 μM (references given by *Tremblay et al.* [2006b]) so it is likely that NO_3^- uptake was substrate-limited at or soon after ice break up. The combination of photoinhibition and low NO_3^- concentrations near the surface would then rapidly shift the maximum growth rates of shade-adapted algae to a deeper portion of the water column. This hypothesis is consistent with the prompt appearance in early June of elevated chlorophyll fluorescence at 30 m at the nearby mooring site (Figure 5). The combined fluorescence data from the rosette and the mooring show that the SCM gained in intensity during June and persisted until at least early August. Note that the variability observed in the mooring record could be due to true variations in the intensity of the SCM, but also to its vertical displacement (e.g., internal waves), and the seasonal deepening of the nitracline (Figure 6).

[30] In spring 2004, early SCMs were common and also present along the shelf break (e.g., station 303; Figure 1), where maxima of up to 10 μg chl L^{-1} occurred between 30 and 40-m depth (not shown). These SCMs were dominated numerically by diatoms, with nearly equal shares of pennate and centric forms (Michel Poulin, personal communication, 2007). Several of the pennates could be categorized as algae that grow in or near the ice. By 6 August, diatoms still dominated the SCM but pennate forms had nearly vanished (Michel Poulin, personal communication, 2007).

[31] The rapid onset of the SCM and its subsequent persistence contrasts with what is observed in the North Atlantic and the Atlantic sector of the Arctic Ocean (e.g., the North Water), where the SCM is a late summer feature that develops after the phytoplankton have exhausted the ample supply of nutrients in surface waters. In this "textbook" scenario, the algae eventually become shade-adapted as a consequence of their growth at the deep nutricline. We propose the reverse for the southeastern Beaufort Sea and hypothesize that the SCM forms early because the lower part of the euphotic zone provides a hospitable environment to already shade-adapted algae with a small supply of NO_3^- near the surface. Whether this is achieved strictly by passive sinking and transient accumulation (i.e., growth rates are highest at the SCM and exceed losses) or it involves some degree of buoyancy regulation or retention by turbulence remains to be determined. Clearly, the SCM is potentially a

primary driver of primary production and biogeochemical fluxes in strongly stratified Arctic waters.

4.3. New Production and NCP During Summer 2004

[32] On the basis of the estimated deficits of NO_3^- (Figure 8) and a molar DIC: NO_3^- drawdown ratio of 7.07 ± 0.35, cumulative NO_3−based new production at the WS in 2004 increased from 1.9 g C m^{-2} on 27 May to 9.7 and 17.9 g C m^{-2} on 16 July and 6 August, respectively. These estimates are maximum values since the winter reference was the water mass where NO_3^- concentrations were highest at any given salinity. Using the low-NO_3^- water mass as a reference instead (e.g., closed symbols and solid lines in Figure 3) would decrease these estimates by ca. 25%. However, the deeper part of this alternate reference profile poorly matched the observed profiles during summer (not shown), implying that the high estimates are the most plausible. We assume that the anomalous water mass of 22 December does not constitute a valid reference for estimating new production since it occupied the WS only once and briefly. However, the eddy-like feature obviously traveled beyond the WS and possibly supported much higher new production where it eventually decayed and died. If we assume that NO_3^- consumption in this water was complete in the upper 25 m and then similar in vertical extent to the WS on 6 August, NO_3−based new production could have been at least two times higher (33.6 g C m^{-2}) than in the bay. This is a minimum estimate since the calculation assumes an aged eddy that no longer pumps nutrients to the surface during spring and summer.

[33] Our estimation of NO_3-based new production so far ignores that a portion of the NO_3^- renewal at the surface was in all likelihood supplied by the oxidation of the NH_4^+ present in surface waters during late fall. The inferred nitrification would have proceeded well within the confines of the euphotic zone (the mean depth of the 1% light level for the 4 stations sampled between 21 June and 6 August was 50 ± 7 m) and the NO_3^- end product should be considered as recycled nitrogen. Assuming uniform nitrification rates of 13.2 ± 0.3 nmol N d^{-1} in the upper 50 m for at least 100 winter days (Figure 4) yields a renewal of about 65 mmol NO_3^- m^{-2}. Since, on 6 August, 72% of the reference inventory in this layer had been consumed, we estimate that ca. 47 mmol NO_3^- m^{-2} or about 22% of the net NO_3^-drawdown was regenerated production. A revised figure for NO_3-based new production would be closer to 14 g C m^{-2} on 6 August. This value can be compared to an estimate of the annual particulate organic carbon (POC) export (6.8 g C m^{-2} at 200 m) at the mooring site (CA-20), 55% of which occurred between July and September [*Forest et al.*, 2008]. The vertical attenuation of C flux between 50 and 200 m in the Arctic is on the order of 47% (North Water Polynya; *Tremblay et al.* [2006a]), which gives a flux of ca. 14.4 g C m^{-2} at 50 m. This estimation is crude but agrees with the estimated NO_3−based new production if steady state is assumed. A comparison of the chlorophyll inventories and net NO_3^- deficits (as a rule of thumb 1 mmol NO_3^- assimilated produces ca. 1 mg of chl *a*) suggests that less than 44 and 15% of the missing nitrogen was present in the phytoplankton standing stock on 21 July and 6 August, respectively, which is consistent with the grazing and sinking losses reported by *Forest et al.* [2008].

[34] At first glance, the close match between the estimated NO_3-based new production and sinking flux at 50 m suggests that very little of the carbon biomass was stored in the biomass of herbivores and DOC during summer, in contrast with observations made in the North Water [*Tremblay et al.*, 2006a]. However, P drawdown in the upper euphotic zone continued after the exhaustion of NO_3^-, a pattern also seen in the Gulf of Amundsen and Mackenzie Shelf [*Simpson et al.*, 2008]. Figure 9d also implies that additional NCP was fueled by this missing P. If we apply the molar DIC:P drawdown ratio (102) observed during early summer, the extra P consumption would support the additional net fixation of 5 g C m^{-2} in the upper 20 m. What has been termed "carbon overconsumption" relative to nitrogen is not a new phenomenon and has been documented in other oceanic regions [*Sambrotto et al.*, 1993]. In these data sets, however, no additional P depletion accompanied the DIC overconsumption once NO_3^- was depleted. It is thus unlikely that the additional depletion of DIC and P in the upper few meters of the euphotic zone was fueled by nitrogen recycling (e.g., NH_4^+), which, contrary to the current paradigm [e.g., *Harrison*, 1980; *Perez et al.*, 2000] would require P recycling to be much slower than that of nitrogen. Additional sources of nitrogen could be provided by dissolved organic nitrogen (DON) or nitrogen fixation at the surface [*Antia et al.*, 1991; *Yamamoto-Kawai et al.*, 2006], although the latter is probably hindered by low temperatures. An unknown fraction of the allochthonous DON supplied by rivers or advection could be used directly (e.g., urea and amino acids) or made available by bacterial attack and photo-ammonification [*Davis and Benner*, 2005; *Vahatalo and Zepp*, 2005; *Simpson et al.*, 2008]. These issues need to be resolved in order to understand how new production and NCP are likely to respond to increasing temperatures and river discharge in the Beaufort Sea.

[35] The deep vertical extent of the seasonal NO_3^-deficit relative to the pycnocline implies that the subsurface chlorophyll maximum (SCM) accounted for a large share of the annual new production in the southeastern Beaufort Sea (Figure 8). Since NO_3^- was depleted from surface waters on 6 July, the already well-defined SCM possibly accounted for ca. 46% of the NO_3-based new production by 6 August. There are few Arctic data with which to compare these estimates, but they contrast with previous reports in two major ways. First, our estimates of new production based on NO_3^- deficit are very low compared to a diatom bloom in the North Water (77 g C m^{-2} [*Tremblay et al.*, 2002b]) and a *phaeocystis* bloom in the Greenland Sea (46 g C m^{-2} [*Smith*, 1993]). The difference is consistent with the relatively strong, upward renewal of NO_3^- in these systems, especially in the North Water. Second, the diatom communities in the southeast Beaufort Sea achieved a much larger portion of their production at low irradiance beneath the upper mixed layer (Figures 6 and 8). Although SCMs also occur in the more productive North Water [*Booth et al.*, 2002], their contribution to the overall nutrient drawdown is relatively small because of the extensive supply of nutrients to the upper euphotic zone. This distinction may have important implications for food webs (e.g., visual predators) and biogeochemical fluxes, especially the elemental stoichiometry of nutrient drawdown, which we now explore.

4.4. Elemental Stoichiometry

[36] The C:N:P ratios of elemental drawdown observed in the present study (112:14:1) were close to the mean Redfield values of 106:16:1 when NO_3^- concentrations were higher than 0.5 μM. Although consistent with the dominance of diatoms at the SCM, the Si:NO_3^- drawdown ratio for Franklin Bay (1.86; Figure 9a) and the southeast Beaufort Sea in general (1.75; *Simpson et al.* [2008]) was much higher than in the North Water (1.0 [*Tremblay et al.*, 2002a]) and in the Barents Sea (ca. 0.5 when diatoms dominate [*Reigstad et al.*, 2002]).

[37] Elevated consumption of Si relative to NO_3^- by diatoms has been ascribed to iron limitation [e.g., *Takeda*, 1998], species-specific differences in optimal Si requirements [*Brzezinski*, 1985], N limitation or low irradiance [e.g., *Martin-Jézéquiel et al.*, 2000]. Iron is unlikely to have been limiting given the perennially low concentrations of NO_3^- at surface and the adjacent reservoir of iron on the shallow Mackenzie Shelf [*Moore et al.*, 2004]. The optimal Si:NO_3^- requirements of diatoms in the sampling region have not been determined in isolation, but in the remote source waters of the eastern and central Bering Sea the Si:NO_3^- drawdown ranges from 1.8 to 2.0 during particularly productive years when diatoms dominate [*Wong et al.*, 2002]. The important contribution of the SCM to seasonal NCP could also have increased the relative consumption of Si, which requires less irradiance than the assimilation of C and N into cellular constituents [*Brzezinski et al.*, 2003; *Brown et al.*, 2006; *Martin-Jézéquiel et al.*, 2000; *Raven*, 1983]. Since the assimilatory reduction of NO_3^- is energetically disadvantageous at very low irradiance, a portion of the Si drawdown may also have been fueled by the recycling of reduced N sources (NH_4^+ or DON) and P in the lower euphotic zone. The formation of highly silicified diatom resting spores at the SCM, which was documented elsewhere in the Arctic [*Booth et al.*, 2002; *Michel et al.*, 2002] may have played a secondary role during July and August. Although we cannot overrule any explanation for the elevated Si:NO_3^- drawdown ratio in Franklin Bay relative to Baffin Bay and the Barents Sea, a combination of high optimal Si requirements for the dominant diatoms and growth under low irradiance at the SCM appears most likely.

[38] Our results clearly imply that in situ biological processes differentially recharged the surface with NO_3^- and P between autumn 2003 and spring 2004. Silica has no known dissolved organic pool in surface waters and the seasonal production of biogenic silica has been shown to be completely exported out of the euphotic zone in other Arctic waters [*Tremblay et al.*, 2002b]. In this view, the southeast Beaufort Sea possibly acts as a particularly efficient silicon trap, contributing to the decreasing Si:NO_3^- of surface waters from the Pacific and rivers as they inexorably flow toward the North Atlantic.

5. Summary and Implications

[39] Until now the concentration of nutrients available to micro-algae at the end of winter in the Beaufort Sea was a matter of speculation. We have shown that during autumn 2003 and winter 2004 the renewal of nutrients in the upper euphotic zone was small because of modest mixing by wind, convection and brine rejection. We hypothesize that other mechanisms of N and P supply play a determinant role in this context. Roughly a third of the NO_3^- reservoir available to phytoplankton in spring 2004 was likely supplied by nitrification above the resilient halocline, but this remains to be confirmed experimentally. The rapid consumption of the small NO_3^- pool prior to and after the break up of the fast ice cover presumably triggered the prompt appearance of a SCM in the halocline. Because of its early appearance and persistence as it progressively pushed the nitracline downward throughout summer, the SCM possibly mediated half of the net NO_3^- consumption. In the resulting NO_3-impoverished upper euphotic zone, additional NCP can be sustained by the large residual pool of P that characterizes Pacific-derived waters. The ensuing depletion of P argues against a freshly regenerated source of N for this additional NCP, pointing instead to an allochthonous source. Testing these hypotheses will require detailed investigations of the importance of nonnitrate forms of allochthonous nitrogen for primary producers, the dynamics of nitrification near the surface, and the ecology of SCMs and their significance to annual primary production, food webs, vertical flux and elemental cycling.

[40] Irradiance clearly affects the timing and rate of primary production in seasonally ice-covered, Arctic waters but our analysis supports the notion that cumulative new and net production are driven primarily by nitrogen loading. It was previously proposed that annual pelagic productivity should increase linearly with the lengthening of the ice-free period due to greater light availability [*Rysgaard et al.*, 1999]. It might be so among regions with similar advective and vertical nutrient loading insofar as (1) the available nitrogen might cycle more times in the euphotic zone and increase regenerated production, (2) SCM communities would have more time to exploit the upward nutrient flux or to deepen the nutricline until their compensation depth is attained (in the sense of *Smetacek and Passow* [1990]), and (3) the cumulative supply of N from the photochemical processes that make nonreadily usable forms of nitrogen available to primary producers is larger. The emerging view, however, is that these processes will not augment primary production to the high levels observed when climatic or oceanic singularities strongly subsidize the upper euphotic zone with nutrients. The intrusion into Franklin Bay of an anticyclonic, eddy-like feature from offshore was associated with a doubling of nutrient concentrations near the surface. This singularity quickly moved along, implying that dynamic instabilities along shelf breaks or ice margins can supply and transport nutrients far from their point of origin. Overall, the response of primary producers to the declining ice cover may depend more on the alteration of nutrient load by atmospheric forcing and freshwater input than on changes in light availability.

[41] **Acknowledgments.** We thank the captains, officers, and crews of the CCGS *Amundsen* for their unrelenting support in the field. We also thank the leader of CASES, L. Fortier, and the project coordinators M. Fortier, M. Ringuette, and J. Michaud for their help and organization skills. We are indebted to C. Nozais, K. Lacoste, and S. Brugel for assisting with the collection of nutrient samples during the winter and to M. Arychuck, P. Collin, M. Davelaar, C. Guignard, O. Owens, and N. Sutherland for DIC analyses. S. Brugel kindly provided the extracted chlorophyll data for the calibration of the fluorometer. This work was supported by grants to JET and NMP by the Natural Sciences and Engineering Research Council of Canada, and is a contribution to the

Canada Research Chair on the Response of Arctic Marine Ecosystems to Climate Change.

References

Antia, N. J., P. J. Harrison, and L. Oliveira (1991), The role of dissolved organic nitrogen in phytoplankton nutrition, cell biology and ecology, *Phycologia*, *30*, 1–89.

Bianchi, M., F. Feliatra, P. Tréguer, M.-A. Vincendeau, and J. Morvan (1997), Nitrification rates, ammonium and nitrate distributions in upper layers of the water column and in sediments of the Indian sector of the Southern Ocean, *Deep Sea Res., Part II*, *44*, 1017–1032, doi:10.1016/S0967-0645(96)00109-9.

Booth, B. C., P. Larouche, S. Bélanger, B. Klein, D. Amiel, and Z. P. Mei (2002), Dynamics of *Chaetoceros socialis* blooms in the North Water, *Deep Sea Res., Part II*, *49*(22–23), 5003–5025, doi:10.1016/S0967-0645(02)00175-3.

Brown, L., R. Sanders, and G. Savidge (2006), Relative mineralisation of C and Si from biogenic particulate matter in the upper water column during the North East Atlantic bloom in spring 2001, *J. Mar. Syst.*, *63*, 79–90, doi:10.1016/j.jmarsys.2006.03.001.

Brzezinski, M. A. (1985), The Si:C:N ratio of marine diatoms: interspecific variability and the effect of some environmental variables, *J. Phycol.*, *21*, 347–357.

Brzezinski, M. A., M.-L. Dickson, D. M. Nelson, and R. N. Sambrotto (2003), Ratios of Si, C and N uptake by microplankton in the Southern Ocean, *Deep Sea Res., Part II*, *50*(3–4), 619–633, doi:10.1016/S0967-0645(02)00587-8.

Carmack, E., and D. C. Chapman (2003), Wind-driven shelf/basin exchange on an Arctic shelf: The joint roles of ice cover extent and shelf-break bathymetry, *Geophys. Res. Lett.*, *30*(14), 1778, doi:10.1029/2003GL017526.

Carmack, E., and R. W. MacDonald (2002), Oceanography of the Canadian shelf of the Beaufort Sea: A setting for marine life, *Arctic*, *55*, suppl. 1, 29–45.

Carmack, E., and P. Wassmann (2006), Food webs and physical-biological coupling on pan-Arctic shelves: Unifying concepts and comprehensive perspectives, *Prog. Oceanogr.*, *71*, 446–477, doi:10.1016/j.pocean.2006.10.004.

Chao, S.-Y., and P.-T. Shaw (1996), Initialization, asymmetry, and spin-down of Arctic eddies, *J. Phys. Oceanogr.*, *26*, 2076–2092, doi:10.1175/1520-0485(1996)026<2076:IAASOA>2.0.CO;2.

Davis, J., and R. Benner (2005), Seasonal trends in the abundance, composition and bioavailability of particulate and dissolved organic matter in the Chukchi/Beaufort Seas and western Canada Basin, *Deep Sea Res., Part II*, *52*(24–26), 3396–3410, doi:10.1016/j.dsr2.2005.09.006.

DOE (1994), *Handbook of Methods for the Analysis of the Various Parameters of the Carbon Dioxide System in Sea Water*, *Version 2*, edited by A. G. Dickson and C. Goyet, ORNL/CDIAC-74, Carbon Dioxide Inf. Anal. Cent., Oak Ridge Natl. Lab., Oak Ridge, Tenn.

Dore, J. E., and D. M. Karl (1996), Nitrification in the euphotic zone as a source for nitrite, nitrate and nitrous oxide at station ALOHA, *Limnol. Oceanogr.*, *41*(8), 1619–1628.

Forest, A., M. Sampei, R. Makabe, H. Sasaki, D. G. Barber, Y. Gratton, P. Wassmann, and L. Fortier (2008), The annual cycle of particulate organic carbon export in Franklin Bay (Canadian Arctic): Environmental control and food web implications, *J. Geophys. Res.*, *113*, C03S05, doi:10.1029/2007JC004262.

Garneau, M. E., W. F. Vincent, L. Alonzo-Saez, Y. Gratton, and C. Lovejoy (2006), Prokaryotic community structure and heterotrophic production in a river-influenced coastal arctic ecosystem, *Aquat. Microbial Ecol.*, *42*(1), 27–40, doi:10.3354/ame042027.

Grasshoff, K. (1999), *Methods of Seawater Analyses*, 600 pp., Weinheim, New York.

Guerrero, M. A., and R. D. Jones (1996), Photoinhibition of marine nitrifying bacteria: 1. Wavelength-dependent response, *Mar. Ecol. Prog. Ser.*, *141*(1–3), 183–192, doi:10.3354/meps141183.

Harrison, W. G. (1980), Nutrient regeneration and primary production in the sea, in *Primary Productivity in the Sea*, edited by P. G. Falkowski, 542 pp., Plenum Press, New York.

Hollibaugh, J. T., N. Bano, and H. W. Ducklow (2002), Widespread distribution in polar oceans of 16S rRNA gene sequence with affinity to Nitrosospira-like ammonia-oxidizing bacteria, *Appl. Environ. Microbiol.*, *68*(3), 1478–1484, doi:10.1128/AEM.68.3.1478-1484.2002.

Johnson, K. M., K. D. Wills, D. B. Butler, W. K. Johnson, and C. S. Wong (1993), Coulometric total carbon dioxide analysis for marine studies: Maximizing the performance of an automated gas extraction system and coulometric detector, *Mar. Chem.*, *44*, 167–187, doi:10.1016/0304-4203(93)90201-X.

Lomas, M. W., and P. M. Glibert (1999), Temperature regulation of nitrate uptake: A novel hypothesis about nitrate uptake and reduction in cool-water diatoms, *Limnol. Oceanogr.*, *44*, 556–572.

Lomas, M. W., and F. Lipschultz (2006), Forming the primary nitrite maximum: Nitrifiers or phytoplankton, *Limnol. Oceanogr.*, *51*(5), 2453–2467.

Marshall, J., and F. Schott (1999), Open-ocean convection: Observations, theory and models, *Rev. Geophys.*, *37*(1), 1–64, doi:10.1029/98RG02739.

Martin-Jézéquiel, V., M. Hildebrand, and M. A. Brzezinski (2000), Silicon metabolism in diatoms: implications for growth, *J. Phycol.*, *36*(5), 821–840, doi:10.1046/j.1529-8817.2000.00019.x.

Mathis, J. T., R. S. Pickart, D. A. Hansell, D. Kadko, and N. R. Bates (2007), Eddy transport of organic carbon and nutrients from the Chukchi Shelf: Impact on the upper halocline of the western Arctic Ocean, *J. Geophys. Res.*, *112*, C05011, doi:10.1029/2006JC003899.

Michel, C., M. Gosselin, and C. Nozais (2002), Preferential sinking export of biogenic silica during the spring and summer in the North Water Polynya (northern Baffin Bay): Temperature or biological control?, *J. Geophys. Res.*, *107*(C7), 3064, doi:10.1029/2000JC000408.

Moore, J. K., S. C. Doney, and K. Lindsay (2004), Upper ocean ecosystem dynamics and iron cycling in a global three-dimensional model, *Global Biogeochem. Cycles*, *18*, GB4028, doi:10.1029/2004GB002220.

Perez, F. F., X. A. Alvarez-Salgado, and G. Roson (2000), Stoichiometry of the net ecosystem metabolism in a coastal inlet affected by upwelling: The Ría de Arousa (NW Spain), *Mar. Chem.*, *69*(3–4), 217–236, doi:10.1016/S0304-4203(99)00107-3.

Peterson, B. J., J. McClelland, R. Curry, R. M. Holmes, J. E. Walsh, and K. Aagaard (2006), Trajectory shifts in the Arctic and Subarctic freshwater cycle, *Science*, *313*(5790), 1061–1066, doi:10.1126/science.1122593.

Pickart, R. S. (2004), Shelfbreak circulation in the Alaskan Beaufort Sea: Mean structure and variability, *J. Geophys. Res.*, *109*, C04024, doi:10.1029/2003JC001912.

Pond, S., and G. L. Pickard (1978), *Introductory Dynamic Oceanography*, Pergamon Press, New York.

Raven, J. A. (1983), The transport and function of silicon in plants, *Biol. Rev.*, *58*(2), 179–207, doi:10.1111/j.1469-185X.1983.tb00385.x.

Reigstad, M., P. Wassmann, C. W. Riser, S. Oeygarden, and F. Rey (2002), Variations in hydrography, nutrients and chlorophyll a in the marginal ice-zone and the central Barents Sea, *J. Mar. Syst.*, *38*, 1–2.

Riedel, A., C. Michel, and M. Gosselin (2006), Seasonal study of sea-ice exopolymeric substances on the Mackenzie Shelf: Implications for transport of sea-ice bacteria and algae, *Aquat. Microbial Ecol.*, *45*(2), 195–206, doi:10.3354/ame045195.

Rysgaard, S., T. G. Nielsen, and B. W. Hansen (1999), Seasonal variation in nutrients, pelagic primary production and grazing in a high-Arctic coastal marine ecosystem, Young Sound, northeast Greenland, *Mar. Ecol. Prog. Ser.*, *179*, 13–25, doi:10.3354/meps179013.

Sambrotto, R. N., G. Savidge, C. Robinson, P. Boyd, T. Takahashi, D. M. Karl, C. Langdon, D. Chipman, J. Marra, and L. Codispoti (1993), Elevated consumption of carbon relative to nitrogen in the surface ocean, *Nature*, *363*, 248–250, doi:10.1038/363248a0.

Simpson, K. G., J. Tremblay, Y. Gratton, and N. M. Price (2008), An annual study of inorganic and organic nitrogen and phosphorus and silicic acid in the southeastern Beaufort Sea, *J. Geophys. Res.*, doi:10.1029/2007JC004462, in press.

Smetacek, V., and U. Passow (1990), Spring bloom initiation and Sverdrup's critical-depth model, *Limnol. Oceanogr.*, *35*, 228–234.

Smith, W. O., Jr. (1993), Nitrogen uptake and new production in the Greenland Sea: The spring Phaeocystis bloom, *J. Geophys. Res.*, *98*(C3), 4681–4688, doi:10.1029/92JC02754.

Takeda, S. (1998), Influence of iron availability on nutrient consumption ratio of diatoms in oceanic waters, *Nature*, *393*, 774–777, doi:10.1038/31674.

Tremblay, J.-É., W. O. J. Smith (2007), Primary production and nutrient dynamics in polynyas, in *Polynyas: Windows to the World*, edited by D. Barber and W. O. J. Smith, pp. 239–263, Elsevier, Berlin.

Tremblay, J.-É., Y. Gratton, E. C. Carmack, C. D. Payne, and N. M. Price (2002a), Impact of the large-scale Arctic circulation and the North Water Polynya on nutrient inventories in Baffin Bay, *J. Geophys. Res.*, *107*(C8), 3112, doi:10.1029/2000JC000595.

Tremblay, J.-É., Y. Gratton, J. Fauchot, and N. M. Price (2002b), Climatic and oceanic forcing of new, net and diatom production in the North Water Polynya, *Deep Sea Res., Part II*, *49*, 4927–4946, doi:10.1016/S0967-0645(02)00171-6.

Tremblay, J.-É., H. Hattori, C. Michel, M. Ringuette, Z.-P. Mei, C. Lovejoy, L. Fortier, K. A. Hobson, D. Amiel, and J. K. Cochran (2006a), Trophic structure and pathways of biogenic carbon flow in the eastern North Water Polynya, *Prog. Oceanogr.*, *71*, 402–425, doi:10.1016/j.pocean.2006.10.006.

Tremblay, J.-É., C. Michel, K. A. Hobson, M. G. Gosselin, and N. M. Price (2006b), Bloom dynamics in early-opening waters of the Arctic Ocean, *Limnol. Oceanogr.*, *51*, 900–912.

Vahatalo, A. V., and R. Zepp (2005), Photochemical mineralization of dissolved organic nitrogen to ammonium in the Baltic Sea, *Environ. Sci. Technol.*, *39*, 6985–6992, doi:10.1021/es050142z.

Wallace, D. W. R., P. J. Minnett, and T. S. Hopkins (1995), Nutrients, oxygen, and inferred new production in the Northeast Water Polynya, 1992, *J. Geophys. Res.*, *100*(C3), 4323–4340, doi:10.1029/94JC02203.

Walsh, J. J., D. A. Dieterle, W. Maslowski, and T. E. Whitledge (2004), Decadal shifts in biophysical forcing of Arctic marine food webs: Numerical consequences, *J. Geophys. Res.*, *109*, C05031, doi:10.1029/2003JC001945.

Ward, B. B. (2002), Nitrification in aquatic systems, in *Encyclopedia of Environmental Microbiology*, edited by D. G. Capone, pp. 2144–2167, John Wiley, Hoboken, N. J.

Wassmann, P., T. Ratkova, I. Andreassen, M. Vernet, G. Pedersen, and F. Rey (1999), Spring Bloom Development in the Marginal Ice Zone and the central Barent Sea, *Mar. Ecol.*, *20*(3–4), 321–346, doi:10.1046/j.1439-0485.1999.2034081.x.

Wells, L. E., M. Cordray, S. Bowerman, L. A. Miller, W. F. Vincent, and J. W. Deming (2006), Archaea in particle-rich waters of the Beaufort Shelf and Franklin Bay, Canadian Arctic: Clues to an allochthonous origin?, *Limnol. Oceanogr.*, *51*(1), 47–59.

Williams, W. J., E. C. Carmack, K. Shimada, H. Melling, K. Aagaard, R. W. Macdonald, and R. G. Ingram (2006), Joint effects of wind and ice motion in forcing upwelling in Mackenzie Trough, Beaufort Sea, *Cont. Shelf Res.*, *26*(19), 2352–2366, doi:10.1016/j.csr.2006.06.012.

Wong, C. S., N. A. D. Waser, Y. Nojiri, F. A. Whitney, J. S. Page, and J. Zeng (2002), Seasonal cycles of nutrients and dissolved inorganic carbon at high and mid latitudes in the North Pacific Ocean during the Skaugran cruises: Determination of new production and nutrient uptake ratios, *Deep Sea Res., Part I*, *49*, 5317–5338, doi:10.1016/S0967-0645(02)00193-5.

Yamamoto-Kawai, M., E. Carmack, and F. McLaughlin (2006), Nitrogen balance and Arctic throughflow, *Nature*, *443*, 43, doi:10.1038/443043a.

Yang, J., J. Comiso, D. Walsh, R. Krishfield, and S. Honjo (2004), Storm-driven mixing and potential impact on the Arctic Ocean, *J. Geophys. Res.*, *109*, C04008, doi:10.1029/2001JC001248.

Yool, A., A. P. Martin, C. Fernandez, and D. R. Clark (2007), The significance of nitrification for oceanic new production, *Nature*, *447*, 999–1002, doi:10.1038/nature05885.

Zhang, X., J. E. Walsh, J. Zhang, U. S. Bhatt, and M. Ikeda (2004), Interannual variability of Arctic cyclone activity, 1948–2002, *J. Clim.*, *17*, 2300–2317, doi:10.1175/1520-0442(2004)017<2300:CAIVOA>2.0.CO;2.

D. Barber, Centre for Earth Observation Science, University of Manitoba, Winnipeg, MB R3T 2N2, Canada.

Y. Gratton, INRS-ETE, 490 de la Couronne, Québec City, QC G1K 9A9, Canada.

J. Martin and J.-É. Tremblay, Département de Biologie, Université Laval, Pavillon Vachon, Québec City, QC G1V OA6, Canada. (jean-eric.tremblay@bio.ulaval.ca)

L. Miller, Institute of Ocean Sciences, Fisheries and Oceans Canada, Sidney, BC V8L 4B2, Canada.

N. M. Price and K. Simpson, Department of Biology, McGill University, 1205 Dr. Penfield, Montréal, QC, H3A 1B1, Canada.